

# RSC Advances



This is an *Accepted Manuscript*, which has been through the Royal Society of Chemistry peer review process and has been accepted for publication.

*Accepted Manuscripts* are published online shortly after acceptance, before technical editing, formatting and proof reading. Using this free service, authors can make their results available to the community, in citable form, before we publish the edited article. This *Accepted Manuscript* will be replaced by the edited, formatted and paginated article as soon as this is available.

You can find more information about *Accepted Manuscripts* in the [Information for Authors](#).

Please note that technical editing may introduce minor changes to the text and/or graphics, which may alter content. The journal's standard [Terms & Conditions](#) and the [Ethical guidelines](#) still apply. In no event shall the Royal Society of Chemistry be held responsible for any errors or omissions in this *Accepted Manuscript* or any consequences arising from the use of any information it contains.



## ARTICLE

# A ZnO Nanowires/PANIPAM Hybrid Energy Converter Driven by Temperature Oscillation

Quanhua Zhang<sup>†</sup>, Ding Wang<sup>†</sup>, Ying Xu, Pengpeng Wang, Xianying Wang\*

Received 00th January 20xx,  
Accepted 00th January 20xx

DOI: 10.1039/x0xx00000x

www.rsc.org/

An inorganic and organic hybrid energy converter consisting of vertically aligned ZnO nanowires (NWs) array and poly N-isopropylacrylamide (PNIPAM) was fabricated. The nanoconverter can generate electric power from the temperature oscillation of environment. The generated voltage is up to 2.1 V and the peak power density is as high as 0.27  $\mu\text{W}/\text{cm}^2$  when the nanodevice is cooled from the room temperature to 8.4 °C. The effective energy conversion performance was attributed to the large deformation coefficient of PNIPAM under cooling stimulation and the piezoelectric effects of ZnO NWs. This work provides an efficient route for the use of alternate energy sources in the environment.

## 1. Introduction

Nanodevices had attracted widespread attention because of their broad applications in nanosensors, UV detectors, and medical implants devices etc.<sup>1-3</sup> Each nanodevice requires a battery to supply electronic power. However, due to large volume, conventional batteries are usually not suitable for these nanodevices. Encouraging progress has been made in the development of nanowires (NWs)-based piezoelectric nanogenerators, which can convert mechanical energy such as wind, friction, and body movement into electric energy in a tiny space.<sup>4-7</sup> However, the key limitation of piezoelectric-based nanogenerators is the requirement of mechanical energy sources, which restricts the use of these nanodevices where a direct mechanical energy source is unavailable.<sup>8</sup> In order to harvest alternate energy sources using nanopiezoelectric materials, it is important to design a new hybrid nanostructure to convert the nonmechanical energy sources such as optical energy, electrical energy, magnetic energy or thermal energy to electricity.<sup>9-13</sup> Chen et al. designed a photon-controlled actuator by using 2-hydroxynaphthylidene-1-naphthylamine (HNAN) and polyvinylidene fluoride-hexafluoropropylene (PVDF-HFP) copolymer membrane, which can be deformed under UV illumination.<sup>14</sup> The deformation converts the optical energy to mechanical energy. And then, electric energy can be obtained because of the piezoelectric property of the embedded nanomaterials.<sup>15</sup> Temperature oscillation is also a common phenomenon in the environment and it is highly desirable if we can change such signal to electricity. In one of our previous work, we designed a nanodevice using ZnO NWs and poly

(vinyl chloride-co-vinyl-co-2-hydroxypropyl acrylate) (PVC) as the basic working unit. ZnO NWs can be deformed while the device was heated because of the swelling of PVC.<sup>8</sup> However, this device can not work when the environmental temperature is dropping. In this work, PNIPAM (poly N-isopropylacrylamide) was chosen as the composite polymer due to its good flexibility and the morphological sensitivity to the decrease of temperature. In contrast to PVC, PNIPAM can swell under cooling stimulations, which makes the embedded ZnO NWs deform quickly because of the mutual interaction.<sup>16,17</sup> As the polymer builds up a strain in the c-axis ZnO NWs, a piezoelectric field can be created along the length direction of ZnO NWs. This novel device here established a methodology for matrix-assisted mechanical-to-electrical energy conversion, which can be used to scavenge energy from a variety of sources including light, heat, pressure, chemical and mechanical.<sup>18</sup>

In this work, vertical ZnO NWs array was prepared via chemical vapor deposition (CVD) method. The morphological and structural characters of ZnO NWs array were analysed through scanning electron microscope (SEM), X-ray diffraction (XRD), Raman and photoluminescence (PL) spectrum. And then, the current-voltage (I-V) characteristics of the nanodevice were measured to study the electrical transporting properties. The performances of energy conversion under temperature stimulation were investigated in detail. At last, the energy conversion mechanism of the nanodevice was explored.

## 2. Experimental

### Fabrication of hybrid ZnO/PNIPAM energy nanoconverter

The schematic diagram and the fabricating process of the device are shown in Fig. 1. Prior to the growth of the c-axis vertical ZnO NWs array, a 3 mm  $\times$  3 mm a-plane sapphire

School of Materials Science and Engineering, University of Shanghai for Science & Technology, Shanghai, 200093, People's Republic of China E-mail: [xianyingwang@usst.edu.cn](mailto:xianyingwang@usst.edu.cn)

<sup>†</sup>These authors contributed equally to the work.

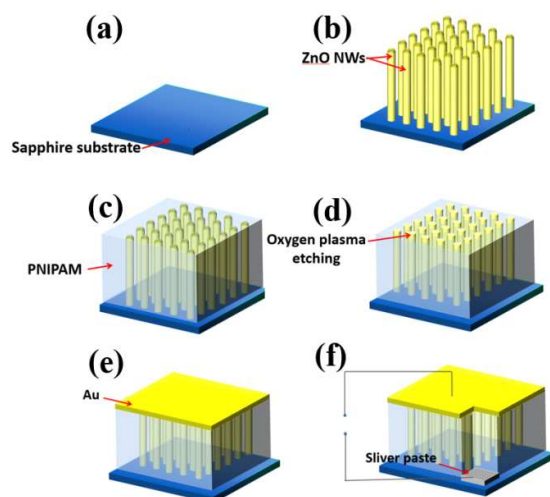


Fig. 1 Fabrication processes of the hybrid ZnO/PNIPAM device. (a) A sapphire substrate deposited with Au catalyst film. (b) Selective growth of ZnO NWs on the substrate. (c) After spin-coating of PNIPAM. (d) The top surface with protruding ZnO NW tips. (e) After coating with Au electrode. (f) Final device with silver paste.

substrate was deposited with a 1.5 nm Au layer as a catalyst (Fig. 1a). As shown in Fig. 1b, the vertically aligned ZnO NWs were epitaxial grown on sapphire substrate via CVD method. The growth temperature and time are 910 °C and 5 min, respectively. And then, PNIPAM was filled into vertical ZnO NWs array by spin-coating and cured at room temperature for 24 h (Fig. 1c). An oxygen plasma etching process was employed to preferentially etch away PNIPAM to expose tips of ZnO NWs (Fig. 1d). The oxygen plasma etching process was carried out on a reactive ion etching system with an operation power of 300 W, an oxygen flow rate of 90 sccm, and etching time of 3 minutes. Then, a 200 nm Au layer was deposited as top contact electrode via electron beam evaporation (Fig. 1e). Afterwards, silver paste was deposited on the underlying ZnO film as the bottom electrode. The final device including silver paste, ZnO, gold and external test circuit is shown in Fig. 1f.

### Characterizations

The morphologies of ZnO NWs were characterized via SEM (FEI, Quanta FEG 450, USA). The crystal structure of the as-grown ZnO NWs was determined by XRD (Bruker, D8 Advance, Germany) with Cu-K $\alpha$  ( $\lambda = 0.15418$  nm) radiation in the range of 10–80° at room temperature. Raman and PL spectra were used to analyze the quality and defect of ZnO NWs (Horiba, LabRAM HR Evolution, France). The Raman characterization was obtained with a He-Ne laser ( $\lambda = 633$  nm) and the PL spectrum was tested using He-Cd laser with a wavelength of 325 nm as the excitation light. Electronic properties of the device were tested using a semiconductor characterization system (Keithley, 4200-SCS, USA).

### 3. Results and discussions

Fig. 2a is a typical SEM image of ZnO NWs, demonstrating that the NWs have consistent vertical growth directions. The inset on the Fig. 2a is an enlarged view of the tip of ZnO NWs.

The average lengths and diameters of the ZnO NWs are about 3  $\mu\text{m}$  and 200 nm, respectively. The alignments of NWs guarantee the same direction of the polarization in all of the ZnO NWs. Raman spectrum was used to examine the crystal qualities of ZnO. As reported, the phonon mode  $E_2$  (high) = 438  $\text{cm}^{-1}$  has a close relationship with ZnO crystal quality, and the peak at 556  $\text{cm}^{-1}$  is associated with oxygen deficiency.<sup>19</sup> As shown in Fig. 2b, a predominant  $A_1$  (TO) mode at 382  $\text{cm}^{-1}$  in the parallel polarization configuration and a predominant  $E_2$  (high) mode at 438  $\text{cm}^{-1}$  in the perpendicular polarization configuration demonstrate the good crystal quality of ZnO NWs. Fig. 2c is the XRD pattern of the vertically aligned ZnO NWs array. The predominant (002) diffraction peak is indicative of c-oriented growth and high degree of vertical alignment. No sharp peaks can be indexed to impurities, indicating a high purity and high crystal quality of ZnO NWs.<sup>20</sup> According to Fig. 2d, band-edge emission in the UV region and green emission can be observed. Green emission is quite weak while the UV emission at 382 nm is strong, indicating high crystal quality of ZnO NWs.<sup>21</sup> These results demonstrate ZnO NWs have high degree of vertical-alignment and good crystal quality. Fig. 2e is the SEM image of the top surface of the nanodevice after oxygen plasma etching. It is obvious that the tips of ZnO NWs are exposed on the PNIPAM polymer surface, which is important for the contact between ZnO NWs and Au electrode.

In order to measure the power generation capability under temperature cycling, a Peltier plate was used to heat or cool the nanodevice. Electrical transport characteristics of the nanodevice were tested using a standard electric probe station equipped with Au micromanipulator probes. The open-circuit voltage ( $V_{oc}$ ) and short-circuit current ( $I_{sc}$ ) were measured to characterize the performance of the nanodevice. From Fig. 2f, it is clear that Schottky contact is formed at the Au-ZnO interface, which is a key component in the operation of the device and it will be discussed in detail.<sup>4, 22</sup>

During the test, the temperature of nanodevice was regulated by a Peltier plate, which was manipulated to be “on” and “off” at 60 s intervals. As shown in Fig. 3, the absolute values of  $V_{oc}$  and  $I_{sc}$  increase with the gradient of temperatures in both the heating and cooling mode. The electrical signals generated from the temperature oscillation are experienced the following processes: First, a strain was formed along the axial direction of the ZnO NWs due to the volumetric change of PNIPAM. Then, the piezoelectric field can be created between the top and bottom of the ZnO NWs. Finally, current can be generated when the Au and Ag electrode were connected by the external circuit. Interestingly, with opposite sign, the value of  $V_{oc}$  and  $I_{sc}$  in the cooling mode is much larger than that in the heating mode with the same temperature interval. The enhanced energy conversion performance can be attributed to the large deformation of PNIPAM under cooling stimulation.<sup>23</sup> The peak value of  $V_{oc}$  and  $I_{sc}$  is up to 2.1 V and 11.5 nA at the temperature range from room temperature to 8.4 °C. Considering the working area (9  $\text{mm}^2$ ) of the nanodevice, a

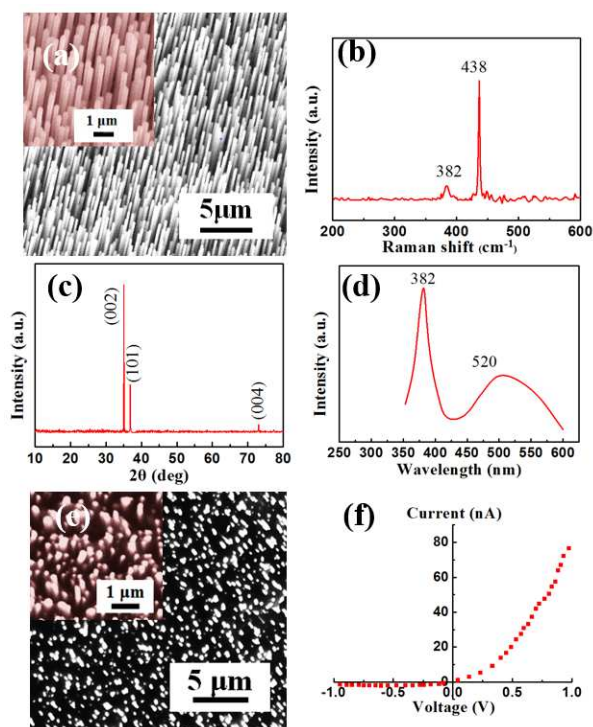


Fig. 2 (a) Tilt view SEM image of the as-grown ZnO NWs. Inset: enlarged view of NW tips. (b) Raman spectrum (c) XRD pattern (d) PL spectra of vertical ZnO NWs arrays. (e) SEM image of the top surface of the device after oxygen plasma etching. (f) I-V curve of the device.

power density of  $\sim 0.27 \mu\text{W}/\text{cm}^2$  was achieved, which is about 14 times higher than the power density of ZnO NWs/PVC nanodevice ( $\sim 19 \text{ nW}/\text{cm}^2$  for temperatures ranging from room temperature to  $65 \text{ }^\circ\text{C}$ ).<sup>8</sup> The great difference between the electric signals under the heating and cooling mode can be explained according to the Schottky contact between Au electrode and ZnO NWs. According to the literature, the top surface of the as-grown ZnO NWs is usually  $\text{O}^{2-}$  terminated.<sup>4</sup> Under the cooling mode, PNIPAM will swell and the embedded ZnO NWs will be stretched, therefore, the top surface of ZnO is negatively charged. In this case, the Au-ZnO barrier is forwardly biased and electrons will flow from ZnO NWs to the Au electrode.<sup>24</sup> On the contrary, the top surface is positively charged under heating mode, the Au-ZnO interface is reversely biased. Thus only very small current can be observed.

The electrical signals have a constant plateau shape rather than a transient spike shape as reported for other devices.<sup>25</sup> This can be explained by the testing circuit of the electric signals, as is shown in the Fig. S1 (in SI). During the test of voltage signal,  $I_{\text{source}}$  was set to “0” and the potential between two ends of the nanowires is directly measured. As the PNIPAM matrix begins to expand and exert stress on the NWs, a piezoelectric potential is generated along the nanowire axis due to the polarization of the  $\text{Zn}^{2+}$  and  $\text{O}^{2-}$  ions in the crystal. Because of the Schottky-like interface and slow neutralization of the strain field in the nanowire, the piezoelectric potential can exist for long periods of time before stress relaxation (tens to hundreds of seconds).<sup>24,26</sup> The NWs remain stressed and the potential will also be kept at a constant value before the device recovers to

room temperature. Therefore, the electrical signals measured have a plateau shape.

The recycling stability of the nanodevice was investigated at cooling temperature of  $\sim 8.4 \text{ }^\circ\text{C}$ . During the test, the Peltier plate was kept “on” and “off” state repeatedly. The temperature dropping rate is about  $3.4 \text{ }^\circ\text{C}/\text{s}$ . From Fig. 4, it can be seen that the value of  $V_{\text{oc}}$  remains unchanged, which reveals that the nanodevice has high repeatability, stability and robustness. The amplified view of a single pulse in the inset of Fig. 4 indicates that the device has the rapid response to the temperature oscillation. As shown in Fig. 1f and Fig. S1, a stress along the axis of the NWs is generated at the cooling status and the NWs will be relaxed when the device temperature is back to the room temperature. The stress of NW is under the circle of “tensile-original status-tensile” instead of “tensile-compressive-tensile”. Therefore, only positive signals are observed. The similar result was also reported by other groups.<sup>4,27</sup>

To verify that the electric signal is generated by the nanodevice rather than the system interference, a switching polarity test was carried out. As is shown in Fig. 5, the ampere meter is connected forwardly (Fig. 5a) and reversely (Fig. 5b), the generated current signals have the same amplitude ( $\sim 11 \text{ nA}$ ), however, the sign is opposite. The inverted output current signals confirm that the current was originated from the nanodevice. For excluding the effect of ZnO pyroelectricity, a control experiment was carried out. In the experiment, the PNIPAM matrix of the nanodevice was selectively removed by acetone. Their voltage response under temperature range of room temperature to  $\sim 8.4 \text{ }^\circ\text{C}$  was also tested. As is shown in the Fig S2 (in SI), compared to the nanodevice with polymer matrix, the generated current of ZnO nanodevice is so small and can be ignored. The pyroelectric voltage is much smaller than the value measured in this work, therefore, pyroelectric effect of ZnO can be ignored.

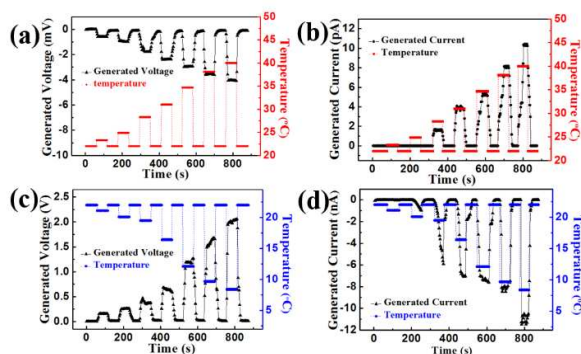


Fig. 3 Generated electric signals of the nanodevice under temperature stimulation. (a) and (b) are  $V_{\text{oc}}$  and  $I_{\text{sc}}$  signals while the device is heated. (c) and (d) are  $V_{\text{oc}}$  and  $I_{\text{sc}}$  signals while the device is cooled.

The energy conversion mechanism of the nanodevice can be extrapolated from both the microstructure of PNIPAM and the piezoelectric effects of ZnO NWs. PNIPAM is the most well-known temperature sensitive polymer.<sup>28</sup> The volumetric change of PNIPAM is attributed to the destruction of the equilibrium between the PNIPAM function groups and the water molecule



in the environment. When heated the device, the PNIPAM chains adopt a compact conformation forming local hydrophobic pockets that significantly discharged the water molecule and reduced the volume.<sup>18</sup> The increase of temperature tends to highlight this volumetric change and increases the intensity of the generated voltage and current (Fig. 3a and Fig. 3b). Different from the heating mode, the PNIPAM-water interactions are stabilized at cooling mode, which lead to the volume expansion.<sup>29</sup> As the polymer expands, a stress along the axis of the ZnO NW is generated. Thus, piezoelectric potential is generated across the NW owing to its piezoelectric effect. Generally, ZnO NW is n-type and the presence of oxygen vacancy and a large portion of surface atoms naturally introduce a moderate conductivity to the NWs. These free carriers can partially screen the piezoelectric charges, but they cannot entirely neutralize the charges.<sup>30</sup> As a consequence, with the stretching and compressing effects of the deformed ZnO NWs, the top and bottom surface was positively and negatively charged respectively (Fig. 5c). As a result, the ZnO nanoconverter can complete the process of thermal-mechanical-electrical conversion.

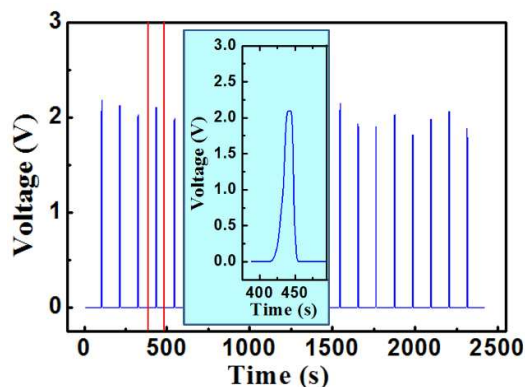


Fig. 4 Voltage response of the nanodevice under repeatedly temperature variation from room temperature to  $\sim 8.4$  °C.

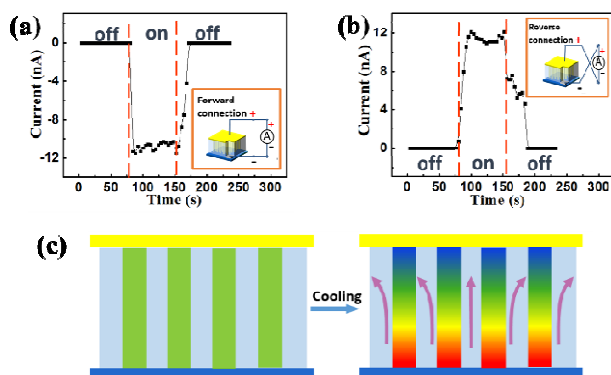


Fig. 5 Leads exchanging experiment carried out from the room temperature to  $8.4$  °C. (a) Forward connection. (b) Reverse connection. (c) Schematic diagram illustrating the steady-state (left) and stressed (right) state of the ZnO NWs embedded in a PNIPAM matrix. As the polymer expands relative to the substrate, a stress along the axis of the NWs is generated.

#### 4. Conclusion

In summary, we have successfully fabricated an energy nanoconverter based on vertical ZnO NWs and PNIPAM composites to convert thermal oscillation to electric power. The electrical properties of the nanodevice reached a peak voltage of  $2.1$  V and current of  $11.5$  nA at the cooling temperature of  $\sim 8.4$  °C, which corresponds to a peak power density of  $\sim 0.27$   $\mu\text{W}/\text{cm}^2$ . The nanodevice also exhibited good performance over a range of times. With the similar idea, the nanodevice can transform various energy sources including light, mechanical, pressure, fluids or chemical by choosing different polymers. So, this research could stimulate a research trend on matrix-assisted piezoelectric nanoenergy converter.

#### Acknowledgments

This work was supported by NNSF of China (51402192, 11402149), the key grant of Chinese Ministry of Education (212057), State Key Laboratory of Heavy Oil Processing (SKLHOP201503) and the Hujiang Foundation of China (B14006).

#### Notes and references

- 1 J. S. Lee, K. Y. Shin, O. J. Cheong, J. H. Kim and J. Jang, *Scientific Reports*, 2015, **5**, 7887-7894.
- 2 Z. Y. Lin, P. Deng, Y. Nie, Y. Hu, L. Xing, Y. Zhang and X. Xue, *Nanoscale*, 2014, **6**, 4604-4610.
- 3 B. Saravanakumar, R. Mohan, K. Thiyagarajan and S. J. Kim, *RSC Advances*, 2013, **3**, 16646-16656.
- 4 Z. L. Wang, *Advanced Functional Materials*, 2008, **18**, 3553-3567.
- 5 Y. Qin, X. Wang and Z. L. Wang, *Nature*, 2008, **451**, 809-813.
- 6 C. L. Hsu, I. L. Su and T. J. Hsueh, *RSC Advances*, 2015, **5**, 34019-34026.
- 7 Z. L. Wang and W. Z. Wu, *Angewandte Chemie International Edition*, 2012, **51**, 2-24.
- 8 X. Wang, K. Kim, Y. Wang, M. Stadermann, A. Noy, A. V. Hamza, J. Yang and D. J. Sirbully, *Nano Letters*, 2010, **10**, 4901-4907.
- 9 X. Wang, S. Xie, J. Liu, S. O. Kucheyev and Y. M. Wang, *Chemistry of Materials*, 2013, **25**, 2819-2827.
- 10 L. Zhang, J.-H. Yang, X.-Y. Wang, X. He, B. Zhao, Z.-H. Tang, G. Yang and H. X. Qiu, *Chinese Physics Letters*, 2011, **28**, 016501.
- 11 Z. L. Wang, *Journal of Physics: Condensed Matter*, 2004, **16**, 829-858.
- 12 Y. Jeong, M. Sim, *RSC Advances*, 2015, **4**, 40363-40368.
- 13 B. Nikoobakht, X. Wang, A. Herzog and J. Shi, *Chemical Society Reviews*, 2013, **42**, 342-365.
- 14 T. Lan, W. Chen, *Angewandte Chemie International Edition*, 2013, **52**, 6496-6500.
- 15 G. Zhu, A. C. Wang, Y. Liu, Y. Zhou and Z. L. Wang, *Nano Letters*, 2012, **12**, 3086-3090.
- 16 W. Wu, X. Wen and Z. L. Wang, *Science*, 2013, **340**, 952-957.
- 17 H. K. Fu, S. W. Kuo, *Polymer*, 2009, **50**, 1246-1250.
- 18 A. Yu, H. Li, H. Tang, T. Liu, P. Jiang and Z. L. Wang, *physica status solidi (RRL) - Rapid Research Letters*, 2011, **5**, 162-164.
- 19 C.-T. Chien, M.-C. Wu, C.-W. Chen, H.-H. Yang, J.-J. Wu, W.-F. Su, C.-S. Lin and Y.-F. Chen, *Applied Physics Letters*, 2008, **92**, 223102.
- 20 Y. Qiu, D. C. Yang, B. Yin, J. X. Lei, H. Q. Zhang, Z. Zhang, H. Chen, Y. P. Li, J. M. Bian, Y. H. Liu, Y. Zhao and L. Z. Hu, *RSC Advances*, 2015, **5**, 5941-5945.
- 21 Y. Chen, X. Wang, S. Xie, J. Liu, H. Cheng, X. Zheng, F. Liu and J. Yang, *Journal of Nanomaterials*, 2012, **2012**, 1-5.
- 22 R. Yang, Y. Qin, L. Dai and Z. L. Wang, *Nature Nanotechnology*, 2009, **4**, 34-39.
- 23 G. Zhu, R. Yang, S. Wang and Z. L. Wang, *Nano Letters*, 2010, **10**, 3151-3155.
- 24 J. Zhou, P. Fei, G. Bao and Z. L. Wang, *Nano Letters*, 2008, **8**, 2725-2730.

## Journal Name

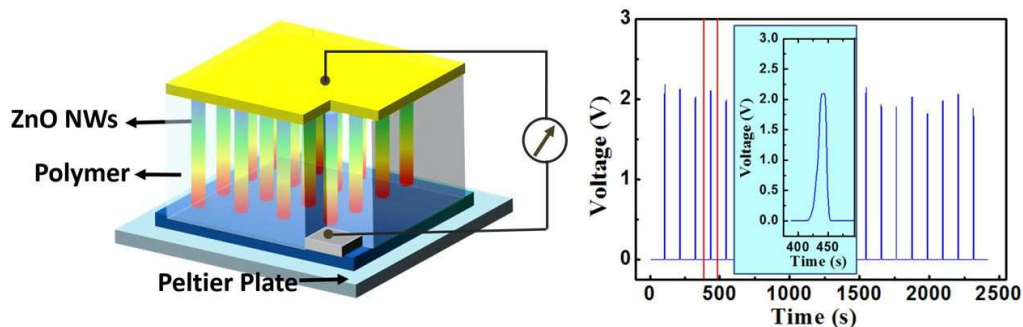
## ARTICLE

- 25 Y. Yang, S. H. Wang, Y. Zhang and Z. L. Wang, *Nano Letters*, 2012, **12**, 6408-6413.
- 26 J. Liu, F. P. J. H. Song, X. D. Wang, C. S. Lao and Z. L. Wang, *Nano Letters*, 2008, **8**, 328-332.
- 27 X. W. Wang, Y. Gu, Z. P. Xiong, C. Zheng and T. Zhang, *Advanced Materials*, 2014, **26**, 1336-1342.
- 28 C. S. Lao, Q. Kuang, Z. L. Wang, M. C. Park and Y. Deng, *Applied Physics Letters*, 2007, **90**, 262107.
- 29 Z. Ahmed, E. A. Gooding, K. V. Pimenov, and S. A. Asher, *Journal of Physical Chemistry*, 2009, **113**, 4248-4256.
- 30 P. X. Gao, J. Song, J. Liu and Z. L. Wang, *Advanced Materials*, 2007, **19**, 67-72.

# Graphical abstract

## A ZnO Nanowires/PANIPAM Hybrid Energy Converter Driven by Temperature Oscillation

Quanhua Zhang<sup>†</sup>, Ding Wang<sup>†</sup>, Ying Xu, Pengpeng Wang, Xianying Wang<sup>\*</sup>



A nano energy converter consisting of vertically aligned piezoelectric ZnO nanowires and temperature-responsive polymer, which can generate electric power while it is cooled down.